U. of Iowa 69-18

The Correlation of Solar Microwave and Soft X-Ray Radiation

2. The Burst Component*

Charles D. Wende**

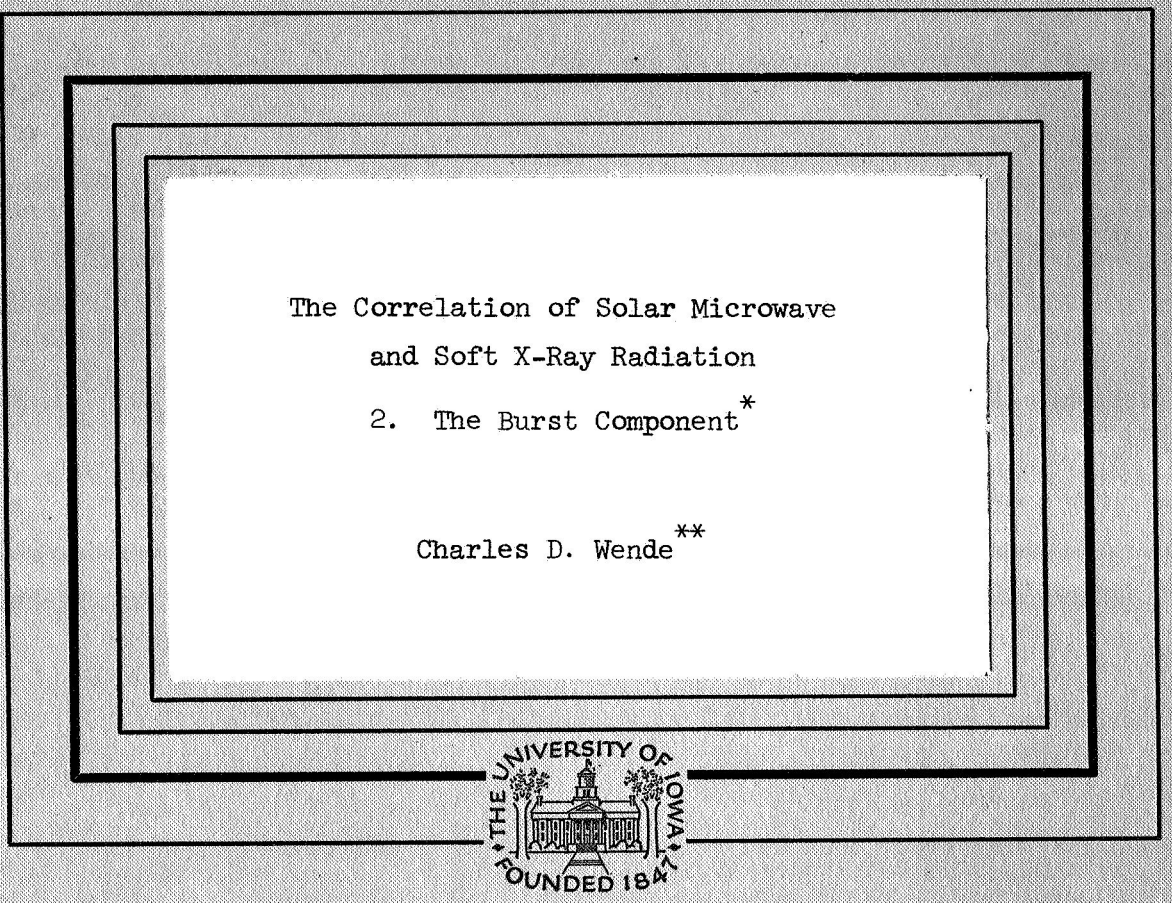

Department of Physics and Astronomy

THE UNIVERSITY OF IOWA

Iowa City, Iowa

U. of Iowa 69-18

The Correlation of Solar Microwave and Soft X-Ray Radiation

2. The Burst Component*

Charles D. Wende**

Department of Physics and Astronomy
The University of Iowa
Iowa City, Iowa 52240

March 1969

*This research was supported in part by the Office of Naval Research under contract Nonr 1509(06), by the National Aeronautics and Space Administration under grant NsG 233-62, by the Jet Propulsion Laboratory under contract JPL 951563, and by the Goddard Space Flight Center of the National Aeronautics and Space Administration under contract NAS5-9076.

**Now at National Space Science Data Center, Goddard Space Flight Center, Greenbelt, Maryland 20771

ABSTRACT

A study of the histories of solar flares observed at 2 cm at the North Liberty Radio Observatory of the University of Iowa and observed at x-ray wavelengths with Mariner V (2-9 A) and Explorers 33 and 35 (2-12 A) shows that "post-burst increase" and "gradual rise and fall" events are concurrent microwave and soft x-ray phenomena. The correlation between the x-ray flux and the radio flux is high but non-linear. The character of the correlation is consistent with a thermal flare theory in which the volume emissivity at x-ray wavelengths is of the spectral form $(dE/d\nu) \sim \exp(-h\nu/kT)$ and the radio flux is from the same region which is optically thick with a temperature T. The correlation yields the peak flare temperature, T_p, and the flare solid angle in terms of the fractional increase in temperature relative to the peak temperature, $F = \delta T/T_p$. Comparing flare sizes with those obtained by other means (e.g., x-ray telescopes) shows $F > 0.2$. If free-free emission is assumed responsible for both the x-ray and the radio emissions, an $F \sim 0.5$ is consistent with the initial assumptions while an $F \sim 1.0$ is not. Thus, temperatures typically double during a flare. Of twenty cases studied, an $F = 0.5$ yielded a mean peak temperature of 4 million degrees Kelvin and a mean effective diameter of 32 arc seconds.

I. INTRODUCTION

Solar radio emissions are conventionally divided into three components, the quiet sun component, the slowly varying component, and the burst component. The x-ray counterparts to the first two components were discussed in part 1 [Wende, 1969]. X-ray flares, or bursts, have been divided into two classes, one of flares originating quasi-thermally and the other of flares originating non-thermally [De Jager, 1965]. The flares that originate non-thermally produce x-rays at wavelengths shorter than about 1 A and are well correlated with impulsive microwave flares such as types simple 1 and simple 2 [Kundu, 1964; Kundu, 1963; Arnoldy et al., 1968]. The quasi-thermal flares produce x-rays at longer wavelengths, have much longer time scales (typically tens of minutes during the decay phase), and are well correlated with sudden ionospheric disturbances, or S.I.D. [Kundu, 1964]. These soft x-ray bursts accompany long enduring microwave bursts of the gradual rise and fall and post-burst increase types [Kawabata, 1966]. This paper is limited to a study of the quasi-thermal bursts.

II. INSTRUMENTATION

The x-ray data were obtained from Geiger tubes flown on the Mariner V (2-9 A), Explorer 33 (2-12 A), and Explorer 35 (2-12 A) spacecrafts. The calibration of these Geiger tubes was discussed in part 1. The x-ray flux, in millierg cm^{-2} sec^{-1} over the specified bandwidth is proportional to the counting rate (after appropriate dead time corrections), and thus counting rate and x-ray flux may be used interchangeably.

The microwave data used in this study were taken by the solar patrol operated by the University of Iowa at the North Liberty Radio Observatory (NLRO). The antenna is an equatorially mounted paraboloid four feet in diameter. The receiver is of a Ryle-Vonberg type in which the antenna noise is balanced against the noise from a gas discharge tube-precision attenuator system. The stepping motor in the servo system limits the thermal resolution to about 4 degrees Kelvin. The radio flux can be given either as a flux density, in watt M^{-2} Hz^{-1}, or as an equivalent antenna temperature in degrees Kelvin. The wavelength of 1.95 cm (a frequency of 15,375 MHz) is such that the normal corona is optically thin and the upper chromosphere is optically thick. The frequency is well above the plasma frequency of any observable region of the solar atmosphere.

III. SIGNIFICANCE OF THE MEASUREMENTS

Before examining the correlation between the soft x-ray flux and the radio flux, it is useful to examine the physical significance of the Geiger tube counting rates and the antenna temperature.

The Geiger tube counting rate is given by:

$$R = \sum_j \int dV \int d\nu \; (dE_j/d\nu) \; \epsilon(\nu) \; (h\nu)^{-1} \; a \; (4\pi \; r^2)^{-1} \; , \qquad (1)$$

where R = the Geiger tube counting rate in counts sec^{-1},

dV = an increment of the volume emitting x rays,

$d\nu$ = the frequency increment,

$(dE_j/d\nu)$ = the energy emissivity of a volume element, in erg cm^{-3} Hz^{-1} sec^{-1},

$\epsilon(\nu)$ = the photon efficiency of the Geiger tube at frequency ν,

h = Planck's constant,

a = the effective area of the Geiger tube in cm^2,

r = the sun-spacecraft distance, and

$\sum_j$ = the summation over all types of emission mechanisms.

Three mechanisms may contribute significantly to the x-ray emission from the sun. They are free-free emission (thermal bremsstrahlung), free-bound emission (radiative recombination), and bound-bound (line) emission.

The volume emissivity for free-free emission is [Karzas and Latter, 1961]:

$$(dE_{ff}/d\nu) = \sum_i CN_e N_i Z_i^2 (h/k) g_{ff} T^{-\frac{1}{2}} \exp(-h\nu/kT) , \qquad (2)$$

where $C = 6.82 \times 10^{-38}$ erg cm^3 deg$^{\frac{1}{2}}$,

N_e = the electron density in cm^{-3},

N_i = the density of ions of effective nuclear charge Z_i, in cm^{-3},

k = Boltzmann's constant,

g_{ff} = the free-free Gaunt factor, of order unity, which the ratio of the actual cross section to the classical cross section,

T = the electron temperature, and

$\sum_i$ = the summation over all ionic species present.

Inserting Eq. (2) into Eq. (1) and integrating yields a free-free contribution for the counting rate of

$$R_{ff} = A_{ff} N^2 V \, T^{\frac{1}{2}} \exp(-\gamma/T) \, , \tag{3}$$

where R_{ff} = the counting rate due to free-free emission,

$N^2 V = \int dV \, N_e^{\,2}$

$A_{ff} = 2.5 \times 10^{-48} \, (N_i/N_e) \, Z_i^{\,2}$, and

γ = 13.58 million degrees Kelvin for Mariner V (2-9 A) and 12.02 million degrees Kelvin for the Explorer detectors (2-12 A).

The volume emissivity of free-bound emission is given by [Elwert, 1952]:

$$(dE_{fb}/d\nu) = C N_e N_{i+1} \, (\chi_H/kT)^{\frac{3}{2}} \, (\chi_{i,n}/\chi_H)(\xi_n/n) g_{fb} \exp((\chi_i - h\nu)/kT) \, , \tag{4}$$

where χ_H = the ionization potential of hydrogen,

$\chi_{i,n}$ = the ionization potential of the final state,

n = the principal quantum number,

ξ_n = the number of places in the nth shell that can be occupied by the captured electron, and

g_{fb} = the free-bound Gaunt factor.

Inserting Eq. (4) into Eq. (1) yields a free-bound contribution to the counting rate of:

$$R_{fb} = A_{fb} N^2 V T^{-\frac{1}{2}} , \tag{5}$$

where R_{fb} = the counting rate due to free-bound emission, and

$A_{fb} = 5.5 \times 10^{-51} \sum_i (N_{i+1}/N_e)(\chi_{i,n}/\chi_H)(\xi_n/n)$.

Line emission due to dielectronic recombination is quite weak and cannot be observed, although dielectric recombination predominates over radiative recombination in determining the ionization balance of the plasma. The photon emissivity due to bound-bound emission from collisionally excited atoms is [Allen, 1965]:

$$(dE_{bb}/d\nu)(h\nu)^{-1} = DT^{-\frac{1}{2}}(f/W_i)N_e N_n \, \delta(\nu - W_i/h) \exp(-W_i/kT) , \tag{6}$$

where $D = 5.1 \times 10^{-4}$,

f = the oscillator strength,

W_i = the excitation energy of the line in eV, and

N_n = the density of ions of principal quantum number n.

The counting rate due to line emission is found by inserting Eq. (6) into Eq. (1). The counting rate due to line emission is

$$R_{bb} = A_{bb} N^2 V T^{-\frac{1}{2}} \exp(-W_i/kT) , \qquad (7)$$

where R_{bb} = the counting rate due to bound-bound emission,

$A_{bb} = 10^{-42} \sum_i' f(N_e/N_H)(N_z/N_e)\epsilon(W_i)$,

N_H = the density of hydrogen atoms in cm^{-3},

N_z = the density of the z stage ion, in cm^{-3}, and

$\sum_i'$ = the summation over all lines.

The observed counting rate is the sum of Eqs. (3), (5), and (7), or

$$R = N^2 V \left(A_{ff} T^{\frac{1}{2}} \exp(-\gamma/T) + A_{fb} T^{-\frac{1}{2}} + A_{bb} T^{-\frac{1}{2}} \exp(-W_i/kT)\right) . \qquad (8)$$

For temperatures of a few million degrees Kelvin, the counting rates due to free-free and bound-bound emission are controlled predominantly by the temperature dependence of the exponential term. The temperature dependence of free-bound emission is quiet weak due to the limits of integration (from $\nu = \chi_i/h$ to ν_{max} of the Geiger tube)

and the additional $\exp(\chi_i/kT)$. The counting rates due to all these mechanisms are linear in N^2V.

If the free-free continuum dominates over both the free-bound continuum and the line emission, the counting rate can be approximated by

$$R \cong A N^2 V \exp(-\gamma/T) , \tag{9}$$

where A = a constant that includes the mean value of $T^{\frac{1}{2}}$.

Equation (9) is a good approximation if the emissivity has the general form of:

$$(dE/d\nu) \sim \exp(-h\nu/kT) . \tag{10}$$

A spectrum made up of a series of lines may also be approximated by Eq. (9). If a black-body spectrum is used, γ can be re-evaluated. It is 17.1 million degrees Kelvin for Mariner V and 14.9 million degrees Kelvin for the Explorer detectors.

The incident radio flux density, S, can be expressed in terms of an equivalent antenna temperature, T_a, through the Rayleigh-Jeans law:

$$S = 2 k T_a \Omega_a/\lambda^2 , \tag{11}$$

where Ω_a = the antenna beam solid angle, and

λ = the wavelength being observed.

The antenna beam solid angle is given by [Krauss, 1966, Eq. 3-15):

$$\Omega_a = \int_{4\pi} P(\theta,\varphi)\, d\Omega , \tag{12}$$

where $P(\theta,\varphi)$ = the relative response of the antenna,

and it has a value of 5.43×10^{-4} steradians. The antenna temperature is given by [Krauss, 1966, Eq. 3-116)

$$T_a = \int_{4\pi} T_b(\theta,\varphi)\, P(\theta,\varphi)\, d\Omega/\Omega_a , \tag{13}$$

where $T_b(\theta,\varphi)$ = the brightness distribution observed by the antenna.

Since this paper is concerned with the size and temperature of emitting regions, which can be found in part from Eq. (13), the antenna temperature will be the preferred system of radio flux

units. The conversion from antenna temperature, in degrees Kelvin, to flux units, in 10^{-22} watt meter^{-2} hertz^{-1} is accomplished by multiplying the antenna temperature by 0.4.

The brightness temperature for a given ray trajectory is derived from the equation of transfer and is [Smerd and Westfold, 1949]:

$$T_b = \int T_b(\tau) \exp(-\tau)\, d\tau \,, \tag{14}$$

where τ = the optical depth given by

$$\tau = \int \varkappa \, ds \,, \tag{15}$$

where $\varkappa$ = the absorption coefficient in cm^{-1}, and

ds = an increment along the ray trajectory.

It is assumed that free-free emission is the source of the observed radio emission (neglecting the impulsive component usually attributed to synchrotron emission). The free-free absorption coefficient determined by Ginzburg [1964] is:

$$\kappa = 0.58\, N_e^{\,2}\, T^{-3/2}\, \omega^{-2} \ln(4.6 \times 10^{5}\, T\, \omega^{-2/3}) , \qquad (16)$$

where ω = the observing frequency in radians sec^{-1}.

At the observing frequency of 15,375 MHz,

$$\kappa = 1.4 \times 10^{-22}\, T^{-\frac{3}{2}}\, N_e^{\,2} \log(220\, T) .$$

Assuming that the relative antenna response, $P(\theta,\varphi)$, is unity over the solar disc, the antenna temperature can be divided into two components, the first due to the non-flaring portion of the sun and terrestrial atmospheric radiation, and the second due to the flaring region. For example,

$$T_a = T_o + (\Omega/\Omega_a)\, T_{bf} , \qquad (18)$$

where T_o = the background component,

T_{bf} = the brightness temperature of the flaring region, and

Ω = the solid angle of the flaring region.

If the flaring region is optically thick ($\tau \geq 1$), then T_{bf} is

simply the electron temperature in that region, and the antenna temperature is proportional to the electron temperature. If the flaring region is optically thin ($T \ll 1$), evaluating Eq. (18) for the case of a volume of hot plasma overlying a cooler mass of plasma at a temperature T_o yields

$$T_{bf} = (T_o + \tau T) , \tag{19}$$

where τ is given by the product of $\varkappa$ from Eq. (17) and the thickness of the hot plasma, L. Inserting Eq. (19) into Eq. (18) reveals that T_a is proportional to $N_e^2 L\Omega$, which with a change of units is equivalent to N^2V. T_a is also proportional to $T^{-\frac{1}{2}}$.

Four simple flare models exist. In all of them it is assumed that the x-ray emissions and the radio emissions emanate from a common volume of gas or at least one that has the same temperature throughout. This volume of gas is characterized by a uniform temperature T, a volumetric emission measure N^2V, and, when viewed from earth, a solid angle Ω.

In model 1, the flaring region is optically thin at 2 cm and the whole body of gas remains at a constant temperature. The x-ray flux should correlate linearly with the radio flux as the variable N^2V is common to both emission mechanisms.

In model 2, the flaring region is optically thick at 2 cm and the whole body of gas remains at a constant temperature. The x-ray and radio fluxes would correlate only if an increase in Ω is accompanied by an increase in N^2V.

In model 3, the flaring region is optically thin at 2 cm and the flaring process is primarily a thermal one. The x-ray and radio fluxes should anticorrelate, i.e., the x-ray flux should increase as the radio flux decreases and vice versa.

In model 4, the flaring region is optically thick at 2 cm and the flaring process is primarily a thermal one. The fluxes should correlate in a logarithmic sense as the radio flux is proportional to T and the x-ray flux is proportional to $\exp(-\gamma/T)$. The type of correlation to be expected is illustrated in Fig. 1. If a black-body rather than a free-free spectrum is used, the general shape is the same. Note that for small temperature changes the correlation is approximately semi-logarithmic or even linear.

The determination of which of the above four models is appropriate is accomplished in the next section. The further development of the model chosen is done in the interpretative section.

IV. OBSERVATIONS

Kawabata [1966] showed that long enduring microwave bursts coincided with soft x-ray bursts.

A survey of 140 simple 1 and simple 2 events listed in Solar Geophysical Data during June and July, 1967 showed that in no case did the soft x-ray flux rise over 300 percent above the x-ray background during an impulsive radio event, and in only 24 cases did the x-ray flux rise over 30 percent above the background flux. This survey showed that the impulsive radio emissions are probably due to a mechanism different than that of the soft x-ray emissions.

Examples of solar bursts in which the soft x-ray and 1.95 cm radio events correlate are illustrated in Figs. 2, 3, 4, and 5. The radio data were integrated over the same intervals during which x-ray data were taken (e.g., a 37.2 second interval every 403 seconds for the Mariner V data), and the radio data points correspond temporally to the x-ray data points. Impulsive radio events which occurred during the bursts but whose fluxes did not correlate with the soft x-ray fluxes are shown with 10 second resolution on inserts. Typically, the soft x-ray event corresponds to the post burst increase event observed at 2 cm, and the peak

of the x-ray event occurs after the impulsive radio events (see Figs. 3, 4, and 5). However, if the impulsive radio event is superimposed upon a gradual rise and fall event, the soft x-ray event typically tracks the gradual rise and fall event (see Fig. 2).

The Geiger tube counting rates (x-ray fluxes) are plotted as a function of the antenna temperatures (radio fluxes) for the bursts illustrated in Figs. 2, 3, 4, and 5 are shown in Figs. 6, 7, 8, and 9, respectively. Additional plots showing correlations between the Geiger tube counting rates and antenna temperatures are shown in Figs. 10, 11, and 12. Although the correlations illustrated in Figs. 8 and 9 are approximately linear, the correlations illustrated on the other figures are definitely non-linear. When plotted semi-logarithmically (i.e., the logarithm of the counting rate versus the antenna temperature), the correlation between the soft x-ray and radio fluxes behaves generally in the manner illustrated in Fig. 1.

A total of 28 sets of data (indexed 1 through 28) were obtained for the 20 events (coded A through T) exhibiting the above correlation. These events are listed in Table I. Table II lists concurrent solar activity and SID's. Seventeen of the twenty events could be attributed to major active regions (McMath plages 8905, 8942, 9145, 9146, 9184, and 9204). In all but one

case an optical flare could be associated with the bursts. S.I.D. occurred concurrently with all of the bursts, and radio events were observed at other frequencies with one exception.

V. INTERPRETATION

In choosing a flare model to apply to the observations, it is preferable to use a model that describes all of the observations rather than just a few. For this reason, although the correlations illustrated in Figs. 8 and 9 are linear, the nonlinearity of the other flux correlations rules out the general applicability of model 1 described in Sec. III. Model 2 is difficult to imagine physically, and will be passed over at this time. Since the fluxes do not anticorrelate, model 3 is eliminated conclusively.

Model 4, in which the correlation between the fluxes has the character illustrated by Fig. 1, is consistent with all the observations. The most general assumptions of this model are that the emissivity has the spectral form

$$(dE/d\nu) \sim \exp(-h\nu/kT) \tag{20}$$

at x-ray wavelengths and that the region is optically thick at a wavelength of 2 cm such that the antenna temperature is proportional to the temperature T. That is,

$$T_a = (\Omega/\Omega_a)\, T + \text{constant} . \tag{21}$$

The slope, Sl, obtained from a graph of the logarithm of the x-ray counting rate plotted as a function of antenna temperature is:

$$Sl = \frac{\partial \ln R/\partial T}{\partial T_a/\partial T} = \frac{\gamma\ \Omega_a}{T^2\ \Omega} \ , \tag{22}$$

where γ and Ω_a are parameters of the measuring equipment and Ω and T are parameters of the flare. It is convenient to define the fractional change in the temperature of the flare, F, in terms of the peak temperature of the flare, T_p, through:

$$F = \delta T/T_p \ , \tag{23}$$

where δT = the change in temperature in degrees Kelvin.

The maximum change in the antenna temperature, δT_{aM}, is given by:

$$\delta T_{aM} = (\Omega/\Omega_a)\ \delta T \ , \quad \text{or} \tag{24a}$$

$$T_{aM} = (\Omega/\Omega_a)\ F\ T_p \ . \tag{24b}$$

Inserting Eq. (24b) into Eq. (22) yields expressions for the peak temperature T_p, the flare solid angle Ω, and the effective diameter

of the flare d. These are:

$$T_p = \frac{\gamma F}{Sl\ \delta T_{aM}} \text{ , in degrees Kelvin,} \tag{25a}$$

$$\Omega = \frac{Sl\ \Omega_a\ \delta T_{aM}^2}{\gamma F^2} \text{ , in steradians, and} \tag{25b}$$

$$d = (Sl\ \Omega_a/1.85 \times 10^{11}\ \gamma)^{\frac{1}{2}}\ (\delta T_{aM}/F) \text{ ,} \tag{25c}$$

in arc seconds .

Since F is always less than unity, the above expressions yield maximum allowable temperatures and minimum allowable sizes when F is set equal to one.

Appropriate values of F must next be determined. An F of order 10^{-1} implies that the temperature did not change appreciably during the flare. However, the smaller the temperature change, the larger the area of the flare. For the 20 flares studied, the mean effective flare diameter (assuming F = 1) is about 16 arc seconds. The upper limit for the size given by Paolini et al. [1968] for a flare observed by OSO IV was 60 arc seconds. Thus F must be greater than 0.27 in order that the d's calculated from Eq. (25c) not exceed 60 arc seconds.

To proceed further, one must specify the exact emission mechanism responsible for the x-ray radiation. For the sake of simplicity, the free-free component is chosen. Assuming (N_i/N_e) and Z_i equal unity, and since for a given value of F the area of the flare is known, Eq. (3) yields an expression for the emission measure, N^2L,

$$N^2L = 7.7 \times 10^{34} T^{-\frac{1}{2}} d^{-2} \exp(\gamma/T) , \qquad (26)$$

where d = the diameter of the flare in arc seconds.

Equation (15) can be cast into the form of:

$$\tau = 1.06 \times 10^{10} R T^{-2} d^{-2} \log(220 T) \exp(\gamma/T) \qquad (27)$$

through the use of Eqs. (26) and (17). Using a typical maximum allowable temperature of 5 million degrees Kelvin, a typical minimum allowable flare diameter of 15 arc seconds and a typical peak counting rate of 10^3 counts sec^{-1}, Eq. (27) was solved for F's of 1.0, 0.75, 0.66, and 0.5. In these cases the flare temperature was infinity times the initial temperature, 4 times, 3 times, and 2 times the initial temperature, respectively. The optical

depths obtained at 2 cm were 0.17, 0.42, 0.62, and 2.0, respectively. It is concluded that flare temperatures typically double during the course of a flare, at least in that region that is responsible for the thermal radio and soft x-ray emissions.

For the twenty bursts studied, the distribution of flare diameters and peak temperatures assuming F = 0.5 is illustrated in Fig. 13. For most of the flares it is not necessary to invoke temperatures higher than about 5 million degrees Kelvin. This result is concordant with a result of Acton [1968]. The assumption that the x-ray spectrum is dominated by the continuum is consistent with the findings of Meekins et al. [1968], but the temperatures they derived were half an order of magnitude higher than those determined in this study. In a photograph taken with an x-ray telescope flown on a rocket, Vaiana et al. [1968] observed a flare composed of two main structures, each several minutes of arc long and about 20 arc seconds across. This structure would yield an effective diameter of about 70 arc seconds, and would allow values of F somewhat smaller than the lower limit of 0.27 derived from the earlier OSO IV observations.

For a flare to satisfy the requirement of a large optical thickness at 2 cm, it must originate from a region with an abnormally high electron density which probably is also characterized

by an abnormally high temperature. For example, if the flaring region had a thickness, L, of 25,000 km, an electron density of 10^{11} cm^{-3}, and a temperature of 4 million degrees Kelvin, from Eq. (17) it had an optical depth of 3.8. The plasma frequency of this region would be about 450 MHz, or well below the 15,375 MHz observing frequency, and plasma effects would be negligible. From Eq. (26), assuming that L was about the same as the effective diameter d, typical values of N_e were 5×10^{10} cm^{-3}. Electrons densities of this order are not unrealistic [cf. Acton, 1968].

The flaring region may contribute a large portion of the quiescent x-ray flux. This possibility has been indicated from observations with pin hole cameras [Friedman, 1964], x-ray telescopes [Reidy et al., 1968; Underwood and Muney, 1968; Underwood, 1968; Vaiana et al., 1968], and slit scan spectrometers [Blake et al., 1965] which show that the major portion of the quiet x-ray flux originates in x-ray plages, the size of the plage becoming smaller as the wavelength observed becomes shorter. Almost all of the radiation at wavelengths shorter than 11 to 15 A is emitted from the hot core region of x-ray plages, which is less than one arc minute in diameter. Similar hot core regions have also been observed in the slowly varying component observed at 2 cm [Nagnibeda, 1968].

The fact that 17 of the 20 observed cases could be attributed to major active regions is consistent with the picture that major active regions that produce flares are contributing substantially to the quiescent x-ray flux. In part 1, it was noted that when these regions disappear behind the limb, the quiescent x-ray flux may drop by a factor of 10. The problem is then posed of determining how much of the major active region is involved in the flaring process. In the 2-12 A region of the spectrum, the size of the hot cores approaches the size of the flare itself. One is led to speculate that the mechanism that gives rise to the correlative radio and soft x-ray events, being thermal in nature, is caused by relatively abrupt perturbations in the temperature history of the plages.

This speculation leads to the problem of determining the amount of the background x-ray flux to be subtracted when plotting the correlation between the soft x-ray flux and the radio flux. If the x-ray events occur in the hot core regions of the x-ray plage which dominate the quiescent x-ray flux, then only a small percentage of the pre-flare background x-ray flux should be subtracted, perhaps as little as 10 percent. If the flaring region contributed very little to the pre-flight x-ray flux, then virtually all of the pre-flare background flux should be subtracted.

For this reason two sets of points are given on the right hand panel of Figs. 6 through 12. The boxed points were determined by subtracting a background of 70 to 100 percent of the pre-flare counting rate. The correlation obtained without subtracting a background flux is shown by solid lines (corresponding to dotted points), and the correlation obtained when a background is subtracted is shown by a dashed line (corresponding to boxed points). Those cases in which 100 percent of the background counting rate were subtracted (e.g., Figs. 6, 11, and 12) may be considered extreme examples. The true curve would be expected to lie between the solid line and the dashed line. As the slope was taken at the peak of the flare, the effect of subtracting or not subtracting a background counting rate was minimized.

VI. CONCLUSION

From the observed non-linear correlation between soft x-ray and microwave flares of the gradual rise and fall and post burst increase types it is possible to determine the peak temperature of the flare and the effective diameter of the flare in terms of a factor F, which is the quotient of the change in temperature divided by the peak temperature. A thermal model of the flare is required with only two assumptions, that $(dE/d\nu) \sim \exp(-h\nu/kT)$ and that the optical depth at radio frequencies is greater than unity. If the additional assumption is made that free-free emission along is responsible for the x-ray emissions, an upper limit on F of 0.5 can be determined. Non-thermal processes were not considered as they were not needed to describe the observations, although a non-thermal model may be valid. In handling the data, it does not seem reasonable to subtract the entire pre-flare x-ray flux as there are grounds for believing that the flaring region may contribute significantly to the quiescent background x-ray flux.

TABLE I: Codes of Events

Event	Date	Index	Space-craft	Time (GMT)	Min. Dia. (Arc Sec)	Max. Pk. Temp. (10^6 deg. K)
A	24-07-67	1	MV	2010-2044	27.7	3.2
		2	E33	2022-2045	22.5	4.9
		3	MV	2057-2218	27.2	3.4
		4	E33	2057-2146	19.9	6.2
B	25-07-67	5	MV	1412-1600	34.7	2.7
		6	E35	1431-1500	20.0	7.8
C	25-07-67	7	MV	1653-1720	19.4	4.7
		8	E35	1648-1723	14.9	8.0
D	25-07-67	9	MV	2028-2109	20.5	4.5
E	29-07-67	10	E35	2144-2203	10.9	9.6
F	31-07-67	11	MV	1454-1608	6.7	4.1
		12	E35	1508-1608	8.3	8.1
G	31-07-67	13	E35	1721-1740	8.8	9.4
H	31-07-67	14	E35	2001-2012	15.8	3.3
I	01-08-67	15	MV	1727-1827	21.1	5.5
		16	E35	1700-1820	14.7	11.1
J	03-08-67	17	E35	1635-1651	15.8	4.1
K	29-08-67	18	MV	2043-2140	12.4	15.7
L	02-09-67	19	MV	2016-2123	9.3	8.0
		20	E35	2051-2120	12.9	4.1
M	11-01-68	21	E35	1708-1725	11.7	10.1
N	14-01-68	22	E35	2024-2044	14.4	10.1
O	16-01-68	23	E35	1542-1605	16.0	3.3
P	29-01-68	24	E35	2221-2231	8.2	24.3

TABLE I (Continued)

Event		Index	Space-craft		Min. Dia. (Arc Sec)	Max. Pk. Temp. (10^6 deg. K)
Q	01-02-68	25	E35	1827-1845	18.1	6.0
R	01-02-68	26	E35	1921-1937	19.1	3.4
S	01-02-68	27	E35	1620-1900	20.9	8.3
T	16-02-68	28	E35	1605-1628	15.6	3.7

NOTE: The abbreviations for the spacecraft are: MV = Mariner V
E33 = Explorer 33
E35 = Explorer 35

TABLE II: Solar Activity during Events A--T

Event	Optical Flares	Source Plage(s)	Radio Events (ESSA Code)	S.I.D.
A	1B	8905	3,21,45	SFD,SPA,SCNA,SWF
B	1B,-N, -N,-N	8905	1,3,4,28 29,45	SFD,SPA
C	1N,-F	8905, 8907	1,2,21,29 45	SPA,SEA,SCNA,SWF
D	1N,-N	8905	20	SFD,SPA,SWF
E	-F,-F	8905	none	SFD,SCNA,SWF
F	1N,-N, -F	8905, 8913	1,3,29	SPA,SFD,SWF
G	-F,-N, -N	8905, 8907	2,22,41	SFD,SPA,SWF,SCNA,SES, SES
H	-F,1N	8905	3,20	SFD,SPA,SCNA,SWF
I	2B,-N, 1N	8905, 8913, 8918	3,4,6,29, 30,45	SPA,SFD,SES,SWF,SEA, SCNA
J	-B	8905	1,3,20,45	SFD,SFD,SWF,SES,SCNA, SEA
K	1B,-F -F	8942	1,3,20,45	SPA,SES,SWF,SEA,SFD, SCNA
L	-F,1N	8957, 8959	3,4,20,29, 40,45	SEA,SWF,SCNA
M	2B	9145	3,4,6,29, 45	SWF,SCNA,SES,SEA,SPA, SFD

TABLE II (Continued)

Event	Optical Flares	Source Plage(s)	Radio Events (ESSA Code)	S.I.D.
N	2B	9146	3,4,21,28, 29,45	SWF,SCNA,SEA,SPA,SES, SFD
O	none	--	4,20,29,45	SPA,SFD
P	--	9184	1,3,29,41,45	SWF,SEA,SPA,SES,SFD
Q	1B,1B	9184	1,3,29,41,45	SWF,SEA,SPA,SES,SFD
R	2B	9184	3,4,29,41, 45,47	SWF,SEA,SPA,SES,SFD
S	2B	9206	3,4,21,29, 41,45,47	SWF,SPA,SFD
T	1N	9204	2,3,4,29,30, 45	SWF,SPA,SES,SFD

ACKNOWLEDGEMENTS

This research was submitted in partial fulfillment of the requirements for the degree of Doctor of Philosophy at the University of Iowa, Iowa City, Iowa. The author is grateful to Prof. J. A. Van Allen for his guidance and support of this work. Thanks are also in order for Profs. S. M. Krimigis and G. Payne for their informative discussions and interest in this project, and for Mr. W. Belleville and the Collins Radio Company in Cedar Rapids, Iowa who constructed the 2 cm receiver and supplied technical help when needed.

This research was supported in part by the Office of Naval Research under contract Nonr 1509(06), by the National Aeronautics and Space Administration under grant NsG 233-62, by the Jet Propulsion Laboratory under contract JPL 951563, and by the Goddard Space Flight Center of the National Aeronautics and Space Administration under contract NAS5-9076. The author was a National Aeronautics and Space Administration trainee during part of the time that this work was in progress.

REFERENCES

Acton, L. W., X-ray and microwave emission of the sun with special reference to the events of July 1961, Astrophys. J., 152, 305, 1968.

Allen, C. W., The interpretation of the XUV solar spectrum, Space Sci. Rev., 4, 91, 1965.

Arnoldy, R. L., S. R. Kane, and J. R. Winckler, Energetic solar flare x-rays observed by satellite and their correlation with solar radio and energetic particle emission, Astrophys. J., 151, 711, 1968.

Blake, R. L., T. A. Chubb, H. Friedman, and A. E. Unzicker, Spectral and photometric measurements of solar x-ray emission below 60 A, Astrophys. J., 142, 1, 1965.

De Jager, C., Solar x radiation, Ann. Astrophys., 28, 125, 1965.

Elwert, G., Uber die ionisations-und rekombinationsprozesse in einem plasma und die ionisationsformel der sonnenkorona, Z. Naturforschg., 7a, 432, 1952.

Friedman, H., Ionospheric constitution and solar control, in Research in Geophysics, edited by H. Odishaw, Vol. 1, p. 157, M. I. T. Press, Cambridge, Mass., 1964.

Ginzburg, V. L., The Propagation of Electromagnetic Waves in Plasmas, p. 422, Addison Wesley, Reading, Pa., 1964.

Karzas, W. J. and R. Latter, Electron radiative transitions in a coulomb field, Astrophys. J. Supp. Ser., IV, 55, 167, 1961.

Kawabata, K-A, On x-ray sources of solar flares, Rept. Ionos. Res. Japan, 20, 118, 1966.

Krauss, J. D., Radio Astronomy, Chap. 3, McGraw Hill, New York, N. Y., 1966.

Kundu, M. R., Centimeter-wave radio and x-ray emission from the sun, Space Sci. Rev., 2, 438, 1963.

Kundu, M. R., Solar Radio Astronomy, Chaps. 7 and 13, University of Michigan Radio Astronomy Observatory report 64-4, Ann Arbor, Mich., 1964.

Meekins, J. F., R. W. Kreplin, T. A. Chubb, and H. Friedman, X-ray line and continuum spectra of solar flares from 0.5 to 8.5 angstroms, Science, 162, 891, 1968.

Nagnibeda, V. G., Properties of sources of the slowly varying component of 2 cm solar radio emission, in Structure and Development of Solar Active Regions, edited by K. O. Kiepenheuer, p. 575, Springer-Verlag, New York, N. Y., 1968.

Paolini, F. R., G. S. Vaiana, R. Giacconi, W. P. Reidy, and T. Zehnpfennig, Spectroheliograms of X-Ray Flares from OSO IV, presented at the Midwest Cosmic Ray Conference, Iowa City, Iowa, March 1, 1968.

Reidy, W. P., G. S. Vaiana, T. Zehnpfennig, and R. Giacconi, Study of x-ray images of the sun at solar minimum, Astrophys. J., 151, 333, 1968.

Smerd, S. F. and K. C. Westfold, The characteristics of radio frequency radiation in an ionized gas, with applications to the transfer of radiation in the solar atmosphere, Phil. Mag., 49, 121, 1949.

Solar Geophysical Data, ESSA Research Laboratory, IER-FB-275, U. S. Government Printing Office, Washington, D. C., 1967.

Underwood, J. H., Solar x rays, Science, 159, 383, 1968.

Underwood, J. H. and W. S. Muney, A glancing incidence solar telescope for the soft x-ray region, Solar Physics, 1, 129, 1967.

Vaiana, G. S., W. P. Reidy, T. Zehnpfennig, L. VanSpeybroeck, and R. Giacconi, X-ray structures of the sun during the importance 1N flare of 8 June 1968, Science, 161, 564, 1968.

Wende, C. D., The correlation of solar microwave and soft x-ray radiation, 1. The solar cycle and slowly varying components, submitted to J. Geophys. Res.

FIGURE CAPTIONS

Figure 1. The relative counting rate, R_r, obtained from x rays emitted by free-free emission from a hydrogen plasma of a given temperature.

Figure 2. A flare observed on 24 July 1967. On the main panels the 2 cm data points correspond temporally to the x-ray data points. The impulsive 2 cm bursts which accompanied the gradual rise and fall x-ray and microwave events are illustrated with a time resolution of 10 seconds on the insert. The three vertical lines on the main panels indicate exactly the times of the three impulsive bursts.

Figure 3. A flare observed on 25 July 1967. On the main panels the 2 cm data points correspond temporally to the x-ray data points. The impulsive bursts which accompanied the post-burst increase x-ray and microwave events are illustrated with a time resolution of 10 seconds on the insert. The times of the impulsive peaks are indicated by the vertical lines on the main panels.

Figure 4. A flare observed on 11 January 1968. On the main panels the 2 cm data points correspond temporally to the x-ray data points. The impulsive microwave bursts which accompanied the post-burst increase x-ray and microwave events are illustrated with a temporal resolution of 10 seconds on the insert. The times of the impulsive peaks are indicated by vertical lines on the main panels.

Figure 5. A flare observed on 29 January 1968. On the main panels the 2 cm data points correspond temporally to the x-ray data points. The impulsive microwave bursts which accompanied the post-burst increase x-ray and microwave events is illustrated with a temporal resolution of 10 seconds on the insert. The time of the impulsive peak is indicated on the main panel by a vertical line.

Figure 6. The soft x-ray--microwave flux correlation of event A, index 4. The x-ray flux is proportional to the Explorer 35 counting rate, and the microwave flux is proportional to the antenna temperature. On the right hand panel, the boxed points and the dashed line indicate the results obtained when about 100 percent of the pre-flare counting rate is subtracted from the data.

Figure 7. The soft x-ray--microwave flux correlation of event B, index 6. The x-ray flux is proportional to the Explorer 35 counting rate, and the microwave flux is proportional to the antenna temperature. On the right hand panel, the boxed points and the dashed line indicate the results obtained when about 70 percent of the pre-flare counting rate is subtracted from the data.

Figure 8. The soft x-ray--microwave flux correlation of event M, index 21. The x-ray flux is proportional to the Explorer 35 counting rate, and the microwave flux is proportional to the antenna temperature. On the right hand panel, the boxed points and the dashed line indicate the results obtained when about 75 percent of the pre-flare counting rate is subtracted from the data.

Figure 9. The soft x-ray--microwave flux correlation of event P, index 24. The x-ray flux is proportional to the Explorer 35 counting rate, and the microwave flux is proportional to the antenna temperature. On the right hand panel, the boxed points and the dashed line indicate the results obtained when about 84 percent of the pre-flare counting rate is subtracted from the data.

Figure 10. The soft x-ray--microwave flux correlation of event C, index 25. The x-ray flux is proportional to the Explorer 35 counting rate, and the microwave flux is proportional to the antenna temperature. On the right hand panel, the boxed points and the dashed line indicate the results obtained when about 100 percent of the pre-flare counting rate is subtracted from the data.

Figure 11. The soft x-ray--microwave flux correlation of event G, index 13. The x-ray is proportional to the Explorer 35 counting rate, and the microwave flux is proportional to the antenna temperature. On the right hand panel, the boxed points and the dashed line indicate the results obtained when about 100 percent of the pre-flare counting rate is subtracted from the data.

Figure 12. The soft x-ray--microwave flux correlation of event I, index 16. The x-ray flux is proportional to the Explorer 35 counting rate, and the microwave flux is proportional to the antenna temperature. On the right hand panel, the boxed points and the dashed line indicate the results obtained when about 100 percent of the pre-flare counting rate is subtracted from the data.

Figure 13. The distribution of the peak temperatures and effective diameters determined from the soft x-ray--microwave flux correlations. An F = 0.5 is consistent with the theory if free-free emission is responsible for both the x-ray and radio emissions. The maximum possible peak temperatures, found by setting F = 1.0, are found by doubling the magnitude of the temperature scale (i.e., from 0 to 30 million degrees Kelvin). The minimum allowable effective diameters are found by halving the diameter scale (i.e., 0 to 30 arc seconds). When two or more observations were made of the same flare, the results were averaged.

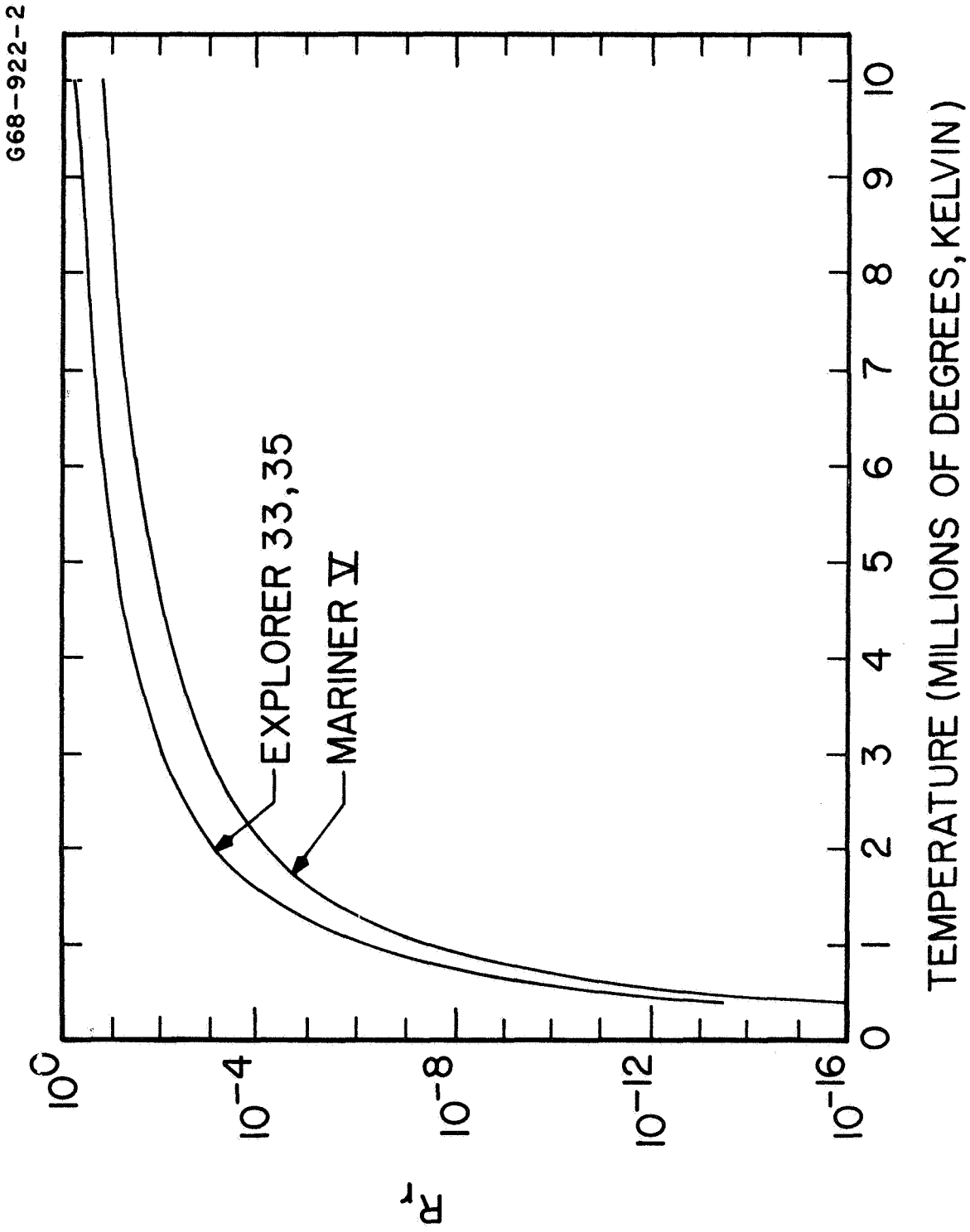
G68-922-2
EXPLORER 33,35
MARINER V
R_r
10^0
10^{-4}
10^{-8}
10^{-12}
10^{-16}
0 1 2 3 4 5 6 7 8 9 10
TEMPERATURE (MILLIONS OF DEGREES, KELVIN)

Figure 1

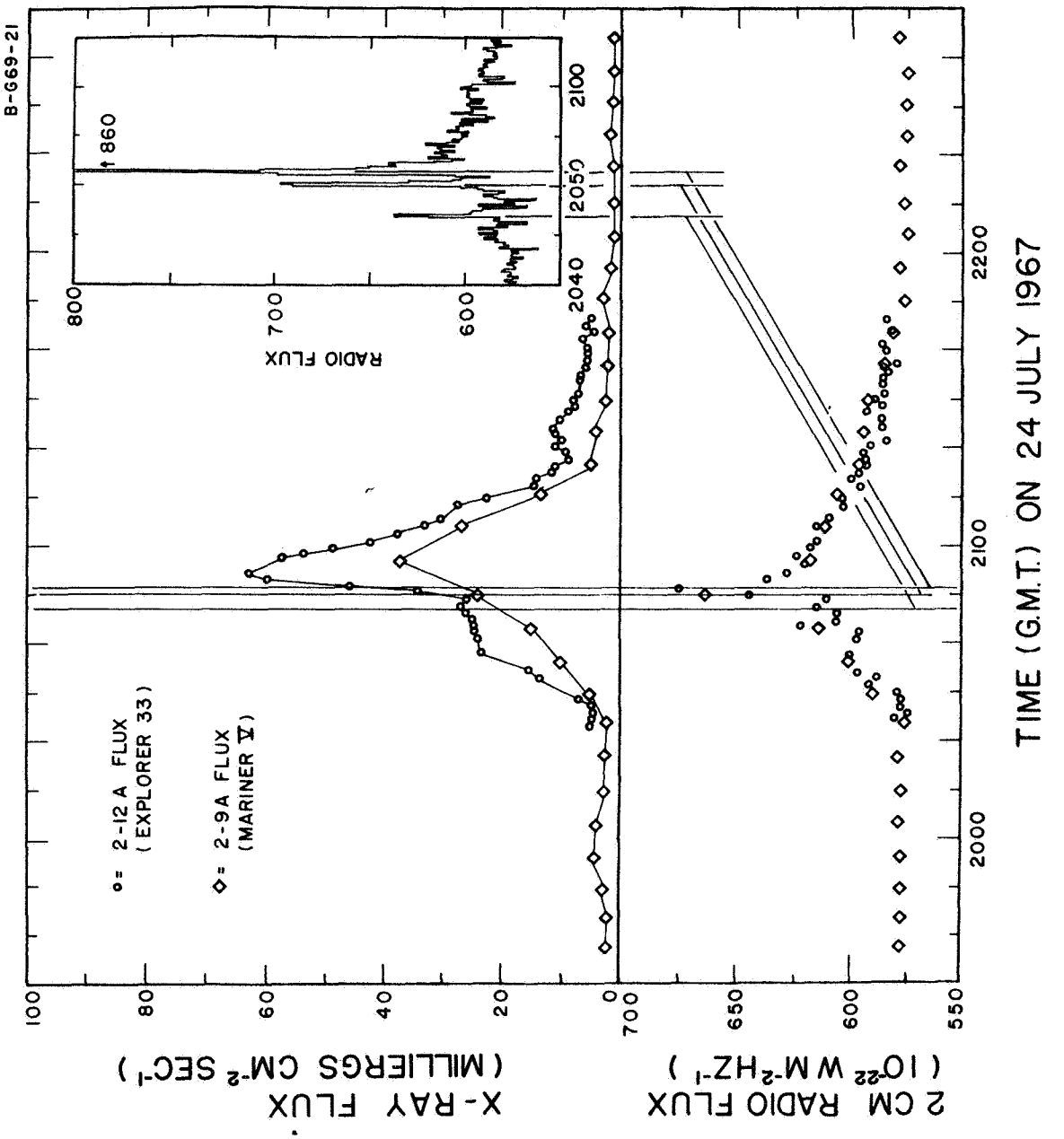
B-669-21
X-RAY FLUX
(MILLIERGS CM⁻² SEC⁻¹)
2 CM RADIO FLUX
(10⁻²² W M⁻² HZ⁻¹)
TIME (G.M.T.) ON 24 JULY 1967
o = 2-12 A FLUX
(EXPLORER 33)
◇ = 2-9A FLUX
(MARINER V)
RADIO FLUX
860

Figure 2

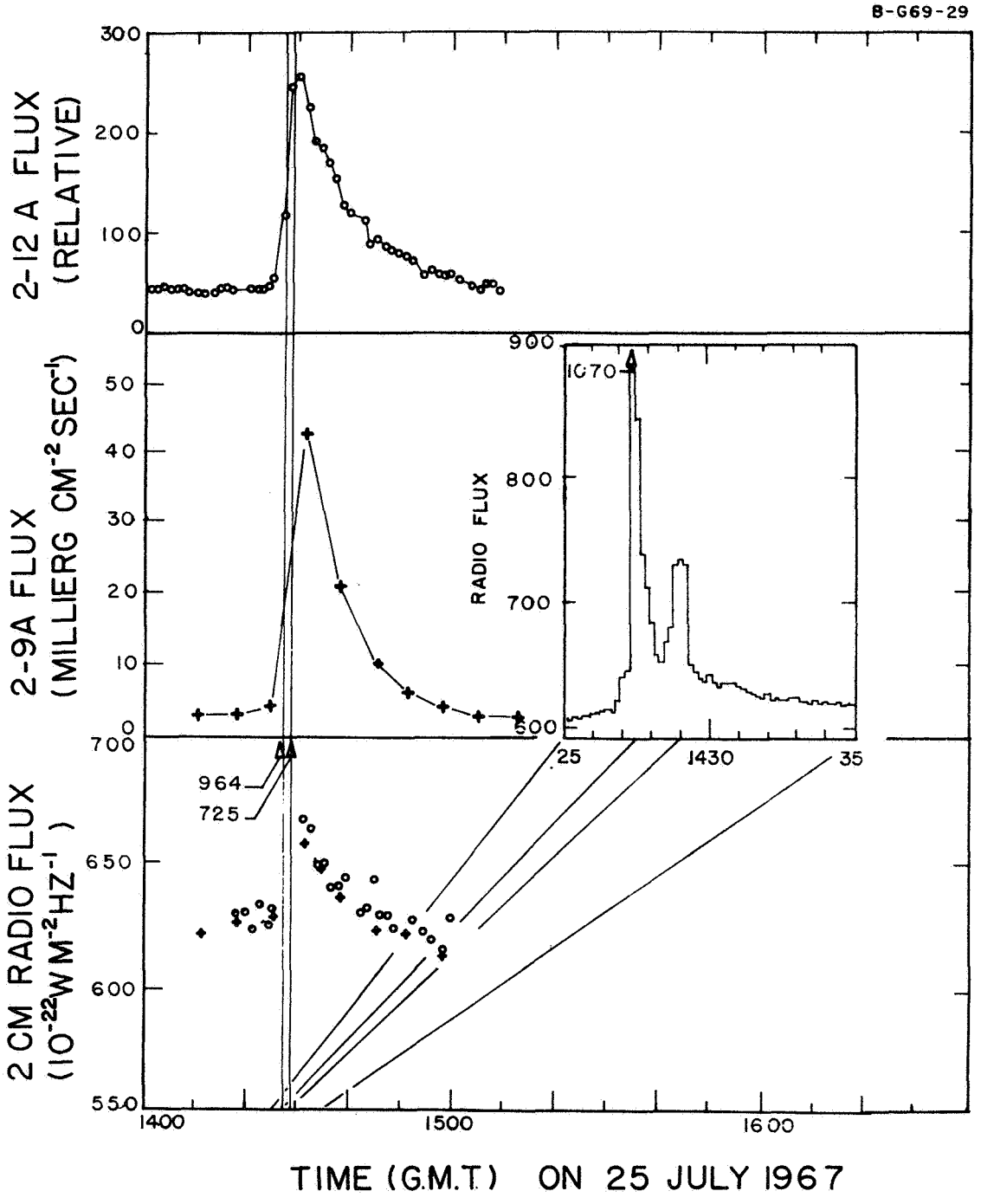
B-G69-29
2-12 A FLUX (RELATIVE)
2-9A FLUX (MILLIERG CM^{-2} SEC^{-1})
2 CM RADIO FLUX (10^{-22} W M^{-2} HZ^{-1})
RADIO FLUX
1070
964
725
25
1430
35
TIME (G.M.T) ON 25 JULY 1967

Figure 3

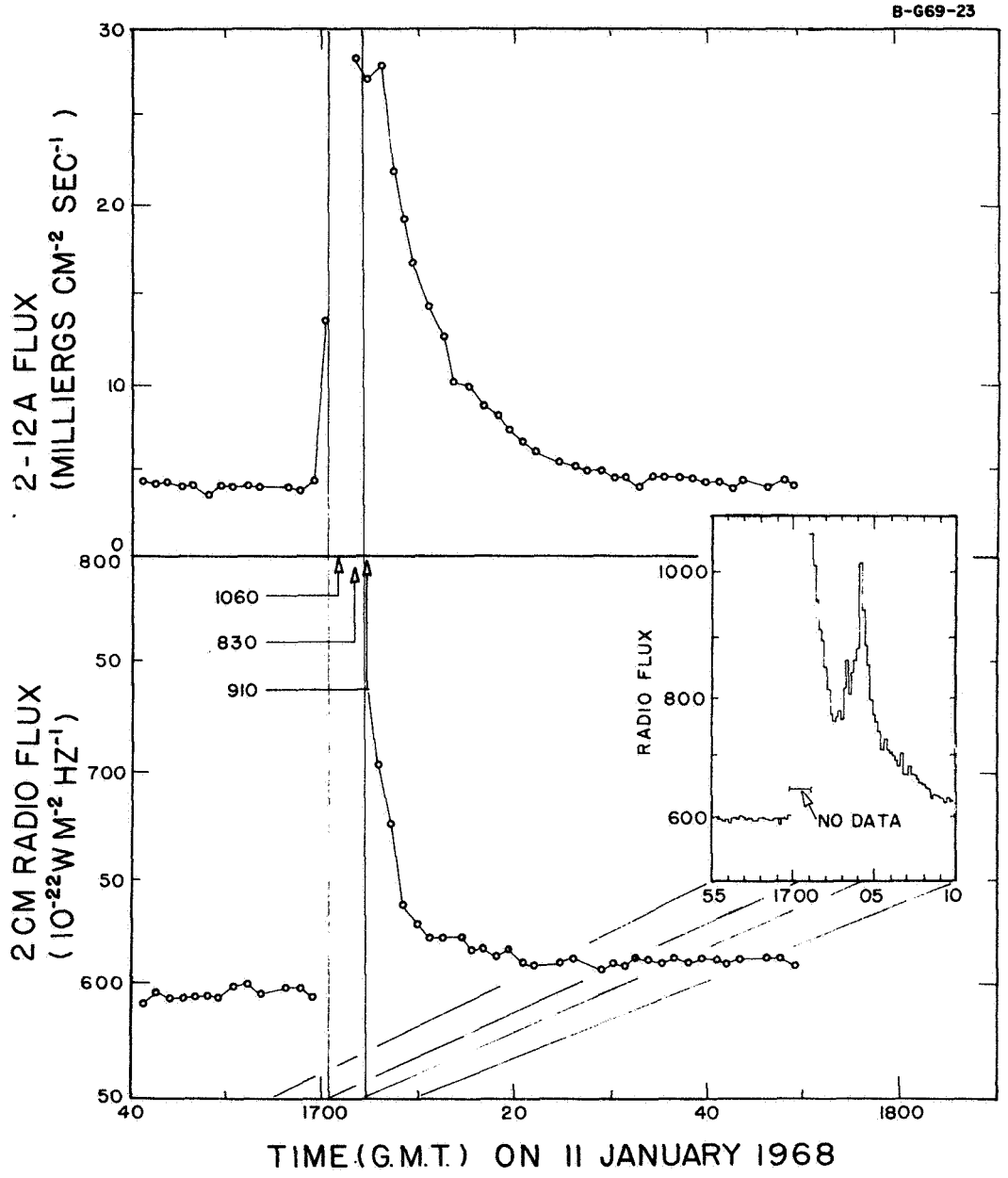
B-G69-23
2-12A FLUX
(MILLIERGS CM-2 SEC-1)
30
20
10
0
2 CM RADIO FLUX
(10-22 W M-2 HZ-1)
800
50
700
50
600
50
1060
830
910
RADIO FLUX
1000
800
600
NO DATA
55
1700
05
10
40
1700
20
40
1800
TIME (G.M.T.) ON 11 JANUARY 1968

Figure 4

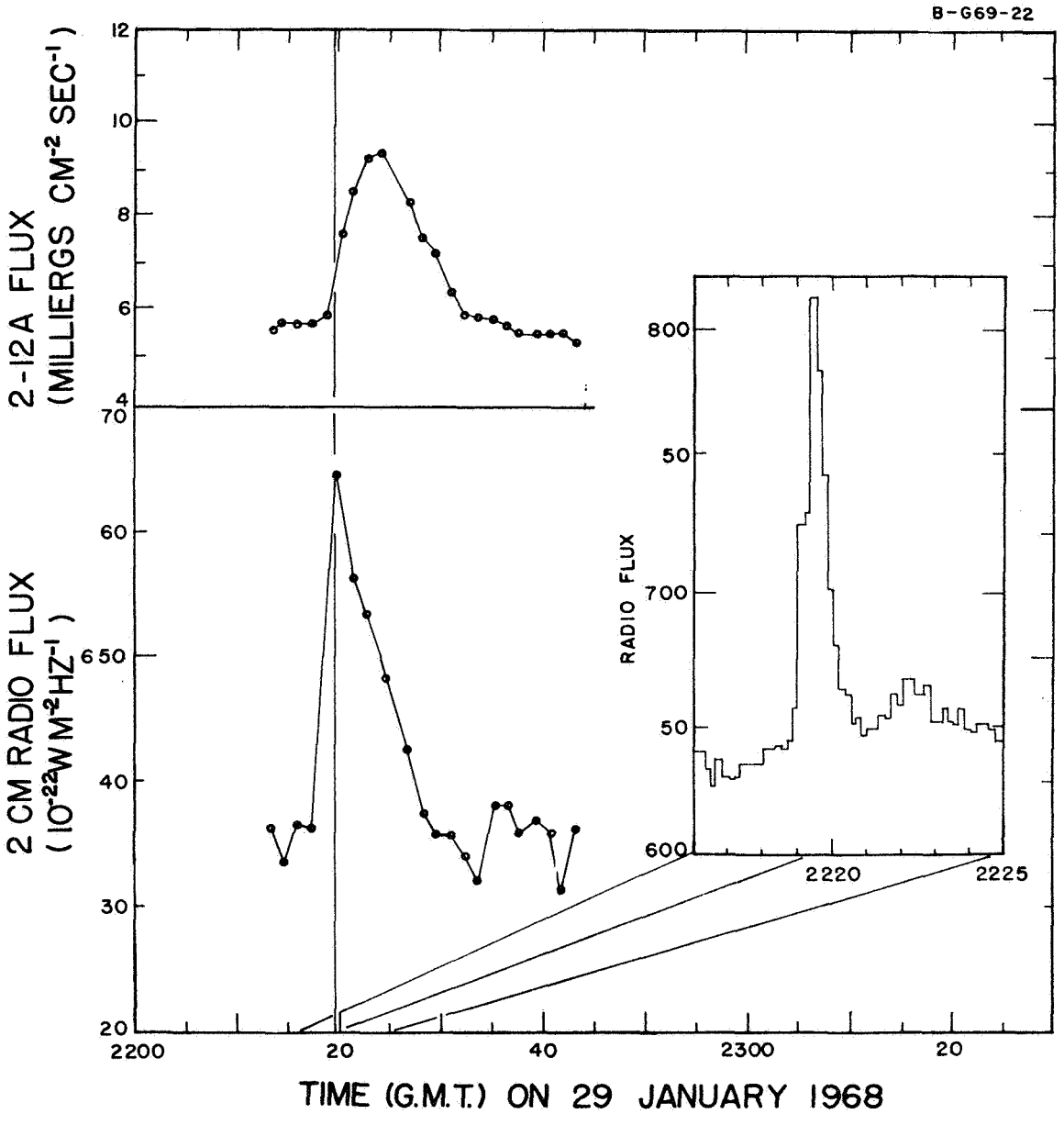
B-G69-22
2-12A FLUX
(MILLIERGS CM-2 SEC-1)
12
10
8
6
4
2 CM RADIO FLUX
(10-22W M-2HZ-1)
70
60
50
40
30
20
RADIO FLUX
800
50
700
50
600
2220
2225
2200
20
40
2300
20
TIME (G.M.T.) ON 29 JANUARY 1968

Figure 5

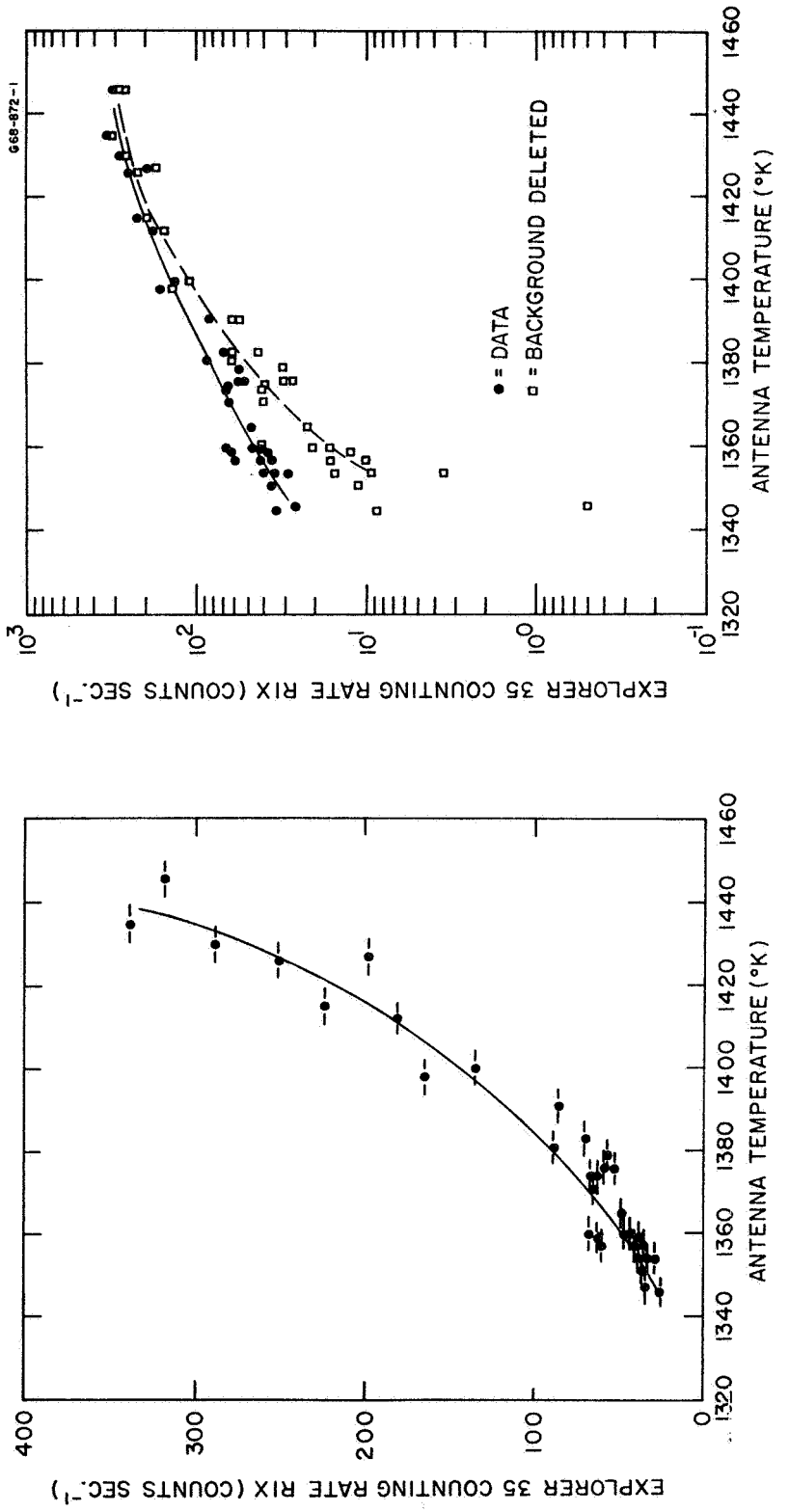
G68-872-1
EXPLORER 35 COUNTING RATE RIX (COUNTS SEC.⁻¹)
10³
10²
10¹
10⁰
10⁻¹
1320
1340
1360
1380
1400
1420
1440
1460
ANTENNA TEMPERATURE (°K)
• = DATA
□ = BACKGROUND DELETED
EXPLORER 35 COUNTING RATE RIX (COUNTS SEC.⁻¹)
400
300
200
100
0
1320
1340
1360
1380
1400
1420
1440
1460
ANTENNA TEMPERATURE (°K)

Figure 6

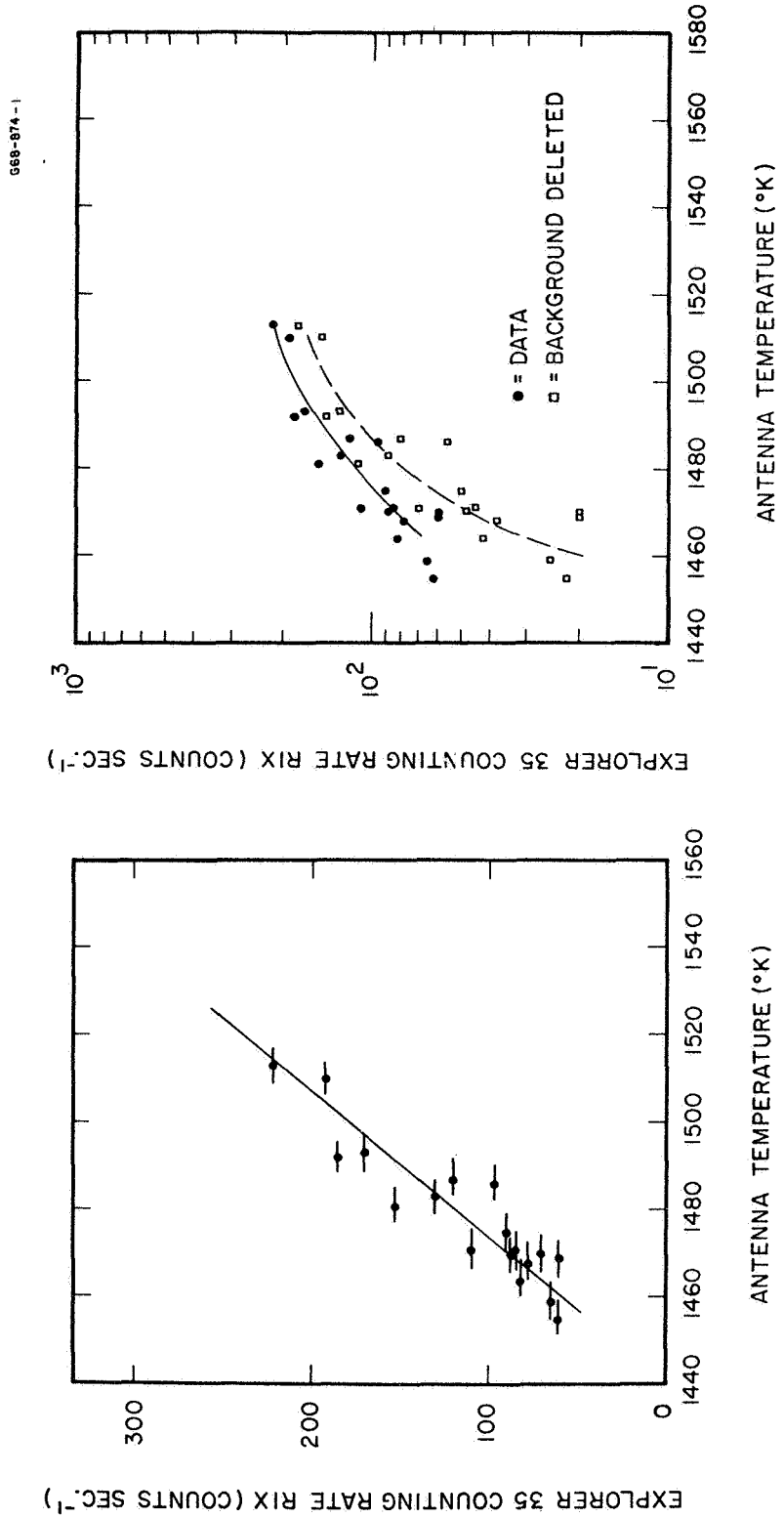
G68-874-1
EXPLORER 35 COUNTING RATE RIX (COUNTS SEC.⁻¹)
ANTENNA TEMPERATURE (°K)
● = DATA
□ = BACKGROUND DELETED
10³
10²
10¹
1440
1460
1480
1500
1520
1540
1560
1580
EXPLORER 35 COUNTING RATE RIX (COUNTS SEC.⁻¹)
ANTENNA TEMPERATURE (°K)
300
200
100
0
1440
1460
1480
1500
1520
1540
1560

Figure 7

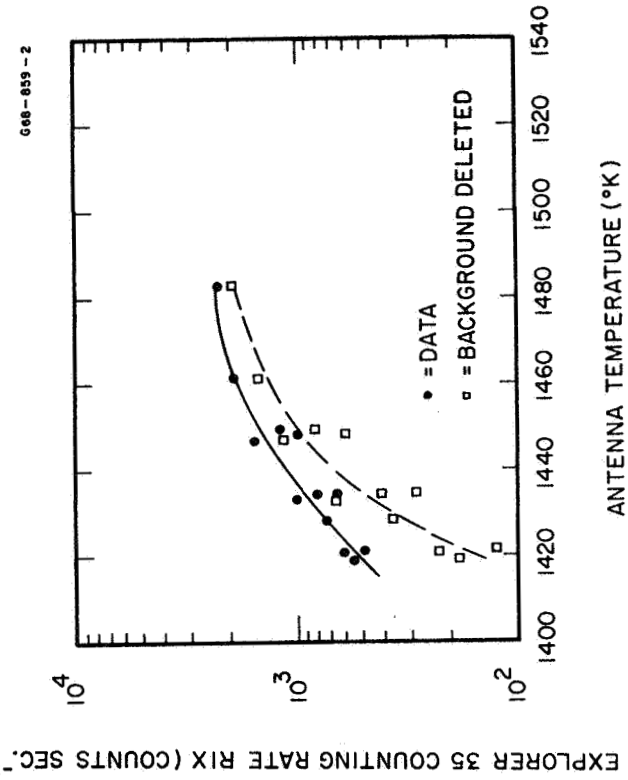
668-859-2
EXPLORER 35 COUNTING RATE RIX (COUNTS SEC.$^{-1}$)
10^4
10^3
10^2
1400
1420
1440
1460
1480
1500
1520
1540
ANTENNA TEMPERATURE (°K)
• = DATA
▫ = BACKGROUND DELETED

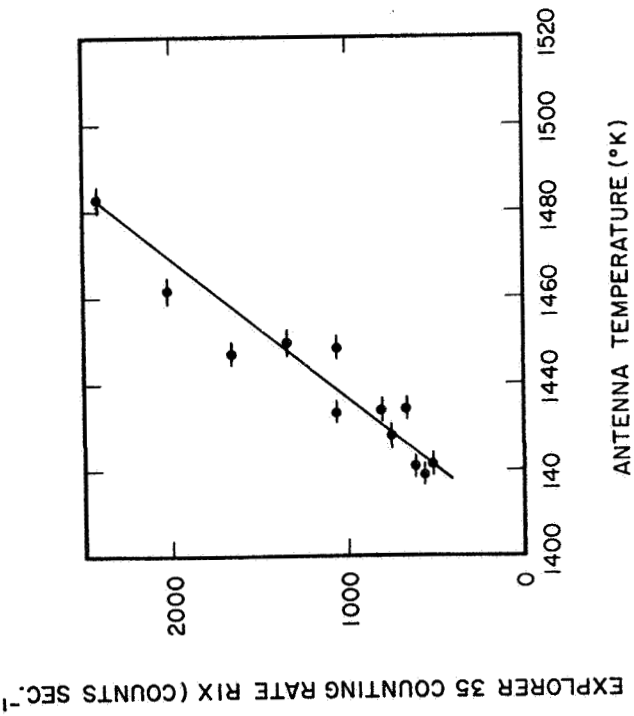
EXPLORER 35 COUNTING RATE RIX (COUNTS SEC.$^{-1}$)
2000
1000
0
1400
140
1440
1460
1480
1500
1520
ANTENNA TEMPERATURE (°K)

Figure 8

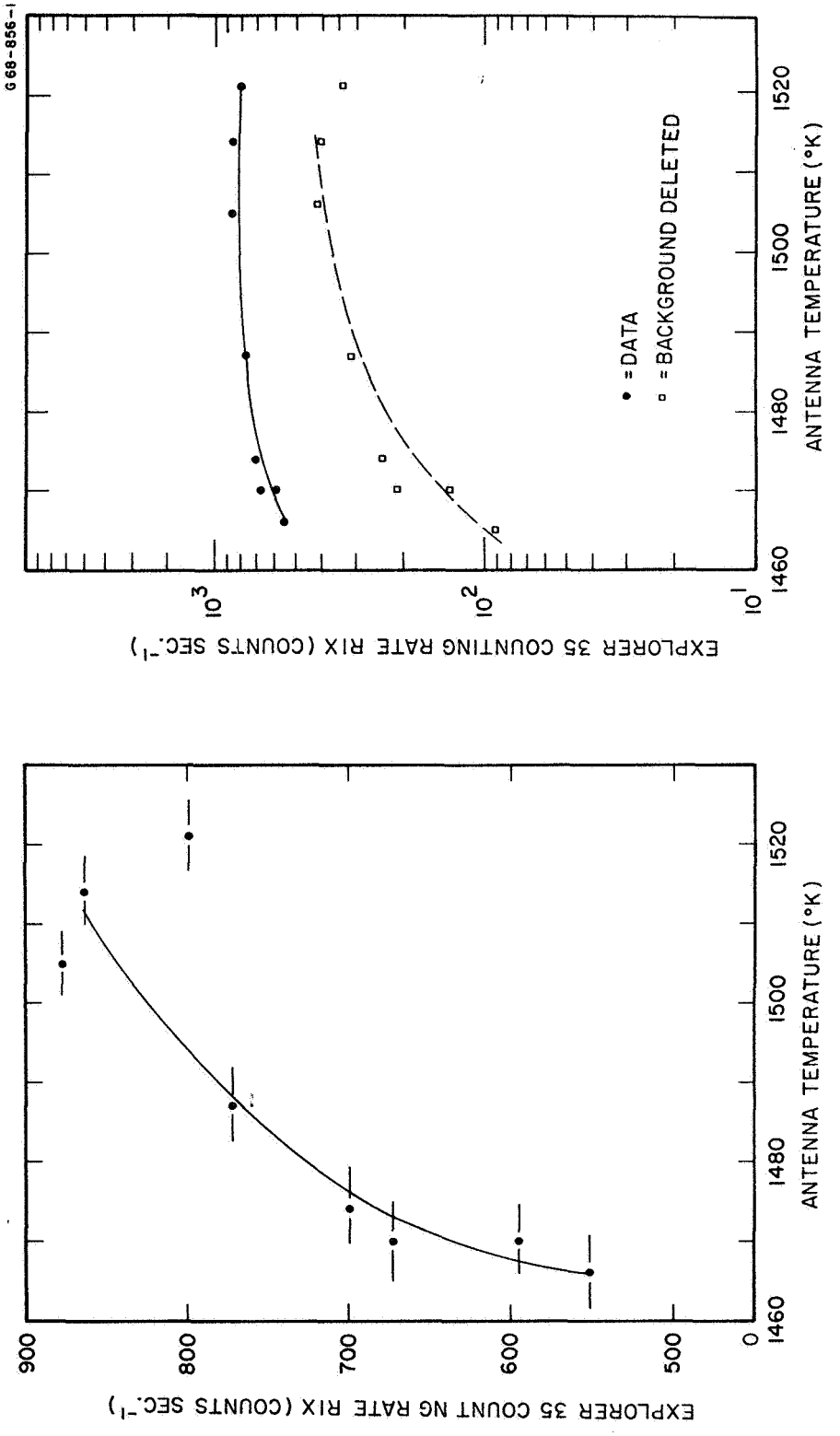
G 68-856-1
EXPLORER 35 COUNTING RATE RIX (COUNTS SEC.$^{-1}$)
10^3
10^2
10^1
1460
1480
1500
1520
ANTENNA TEMPERATURE (°K)
• = DATA
▫ = BACKGROUND DELETED
EXPLORER 35 COUNTING RATE RIX (COUNTS SEC.$^{-1}$)
900
800
700
600
500
0
1460
1480
1500
1520
ANTENNA TEMPERATURE (°K)

Figure 9

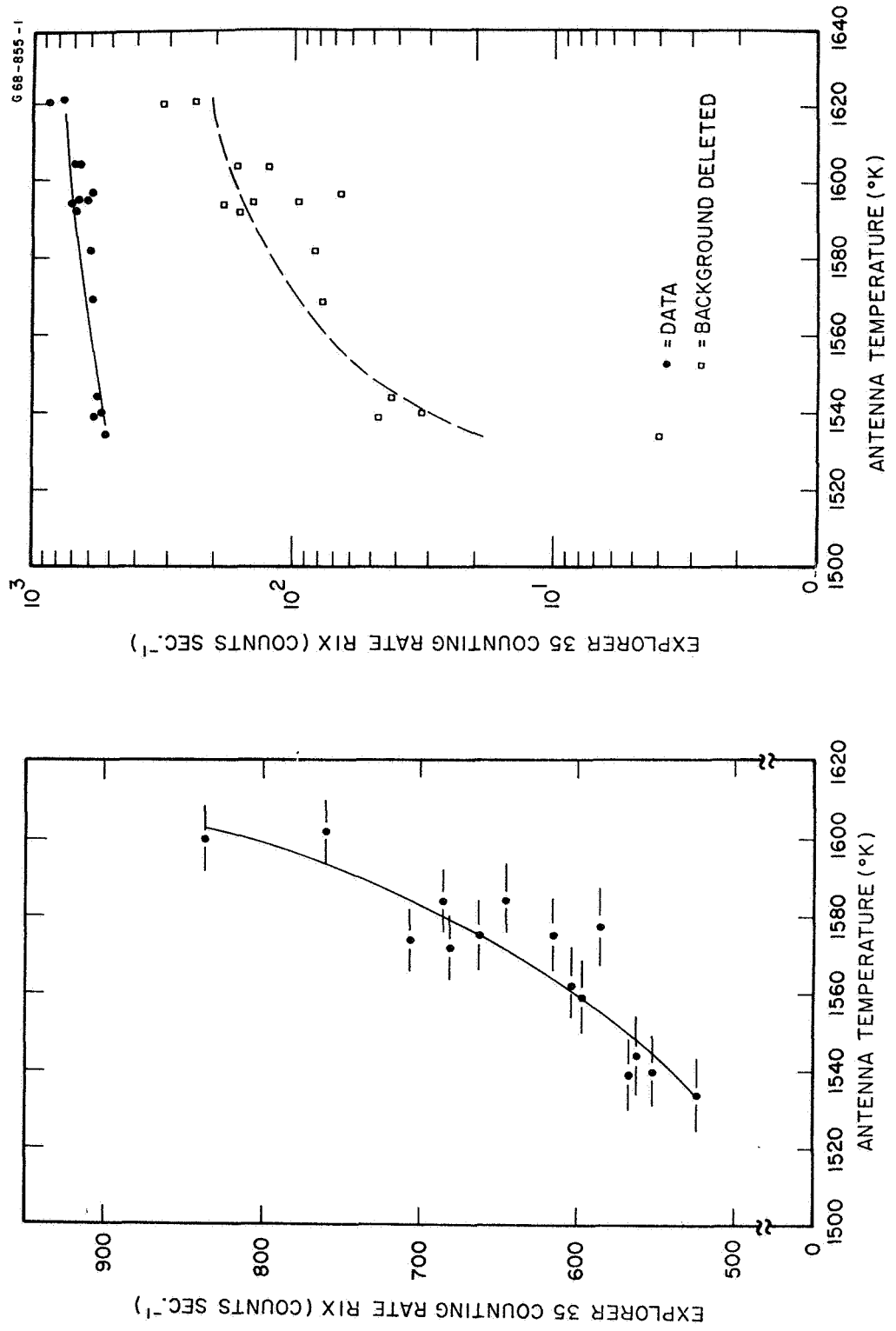
G68-855-1
EXPLORER 35 COUNTING RATE RIX (COUNTS SEC.⁻¹)
ANTENNA TEMPERATURE (°K)
• = DATA
▫ = BACKGROUND DELETED
EXPLORER 35 COUNTING RATE RIX (COUNTS SEC.⁻¹)
ANTENNA TEMPERATURE (°K)

Figure 10

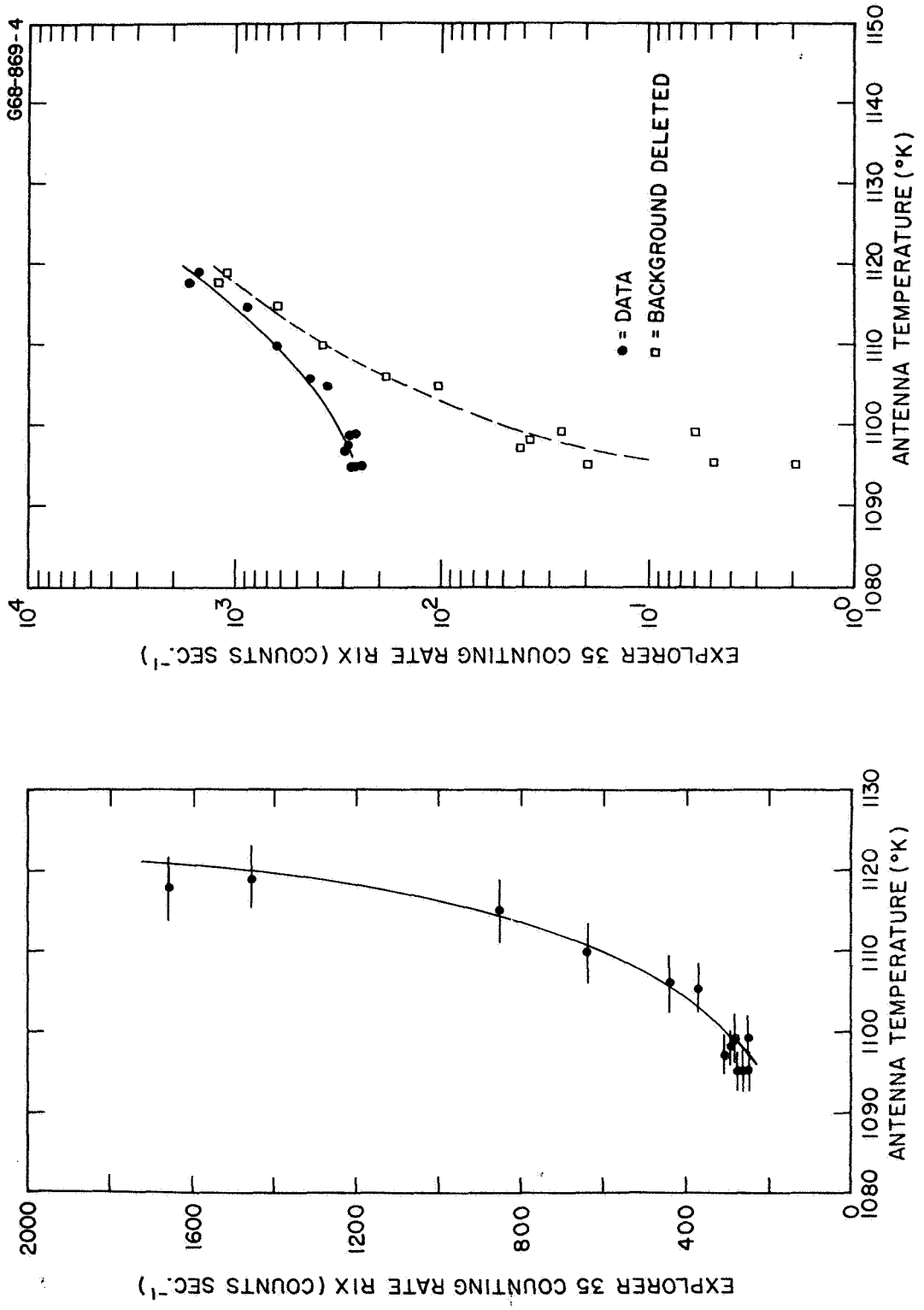
G68-869-4
EXPLORER 35 COUNTING RATE RIX (COUNTS SEC.⁻¹)
ANTENNA TEMPERATURE (°K)
• = DATA
□ = BACKGROUND DELETED
EXPLORER 35 COUNTING RATE RIX (COUNTS SEC.⁻¹)
ANTENNA TEMPERATURE (°K)

Figure 11

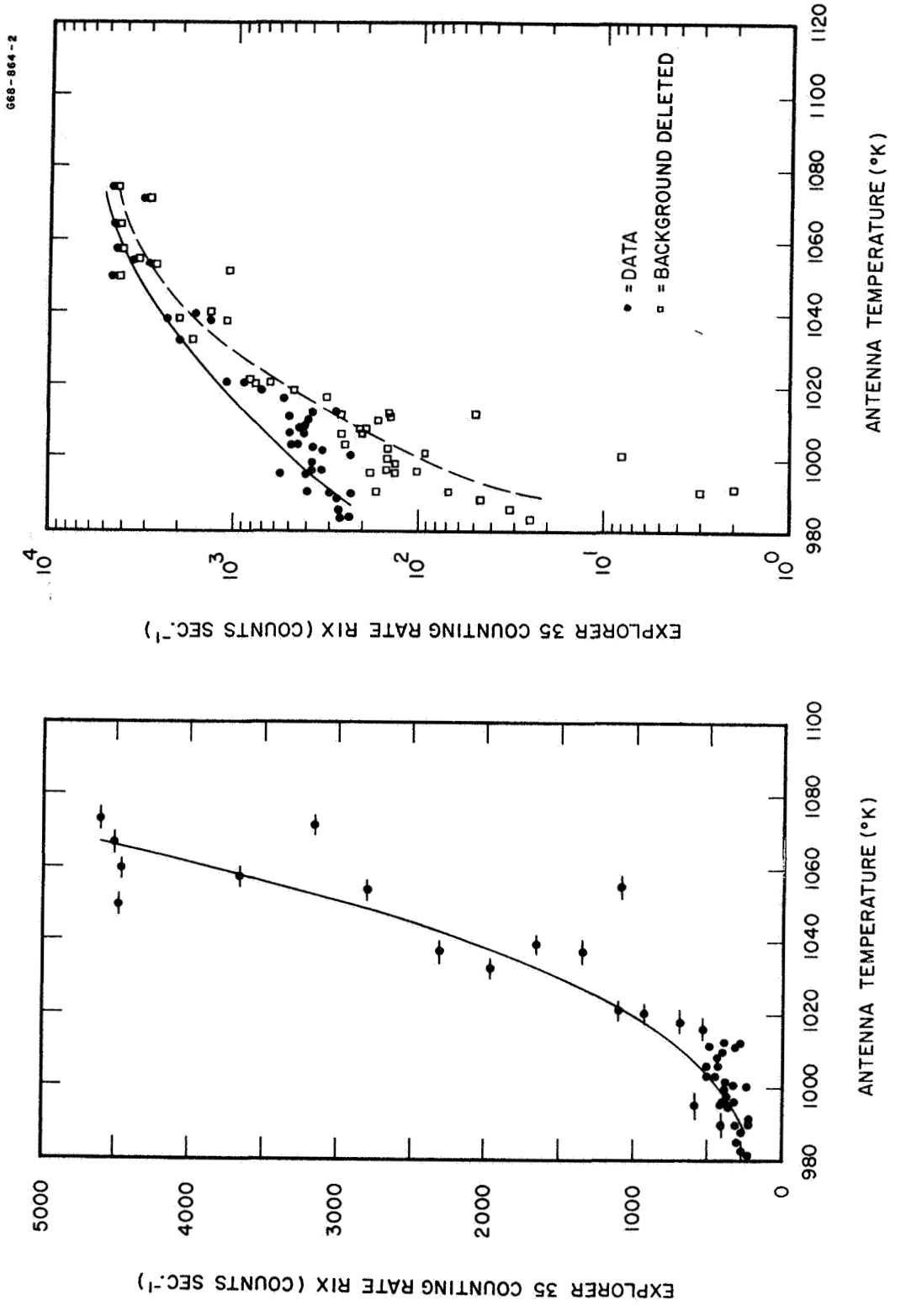
G68-864-2
EXPLORER 35 COUNTING RATE RIX (COUNTS SEC.⁻¹)
ANTENNA TEMPERATURE (°K)
• = DATA
▫ = BACKGROUND DELETED
EXPLORER 35 COUNTING RATE RIX (COUNTS SEC.⁻¹)
ANTENNA TEMPERATURE (°K)

Figure 12

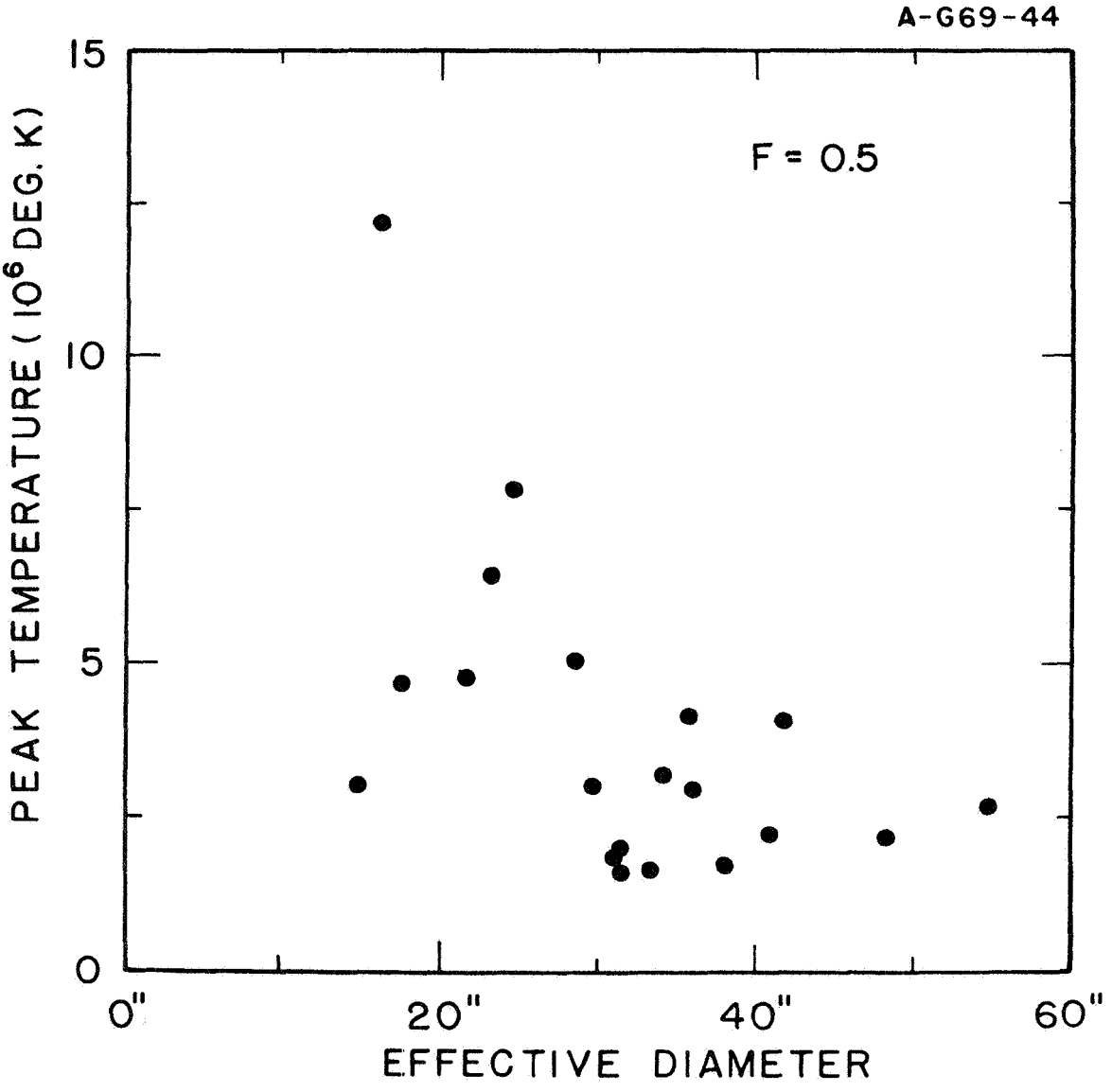
A-G69-44
F = 0.5
PEAK TEMPERATURE (10^6 DEG. K)
15
10
5
0
0"
20"
40"
60"
EFFECTIVE DIAMETER

Figure 13

UNCLASSIFIED

Security Classification

DOCUMENT CONTROL DATA - R&D

(Security classification of title, body of abstract and indexing annotation must be entered when the overall report is classified)

1. ORIGINATING ACTIVITY *(Corporate author)*

Department of Physics and Astronomy
The University of Iowa

2a. REPORT SECURITY CLASSIFICATION

UNCLASSIFIED

2b. GROUP

3. REPORT TITLE

The Correlation of Solar Microwave and Soft X-Ray Radiation

2. The Burst Component

4. DESCRIPTIVE NOTES *(Type of report and inclusive dates)*

Progress Report March 1969

5. AUTHOR(S) *(Last name, first name, initial)*

Wende, Charles D.

6. REPORT DATE	7a. TOTAL NO. OF PAGES	7b. NO. OF REFS
March 1969	53	23

8a. CONTRACT OR GRANT NO. 1509(06)	9a. ORIGINATOR'S REPORT NUMBER(S)
b. PROJECT NO.	U. of Iowa 69-18
c.	9b. OTHER REPORT NO(S) *(Any other numbers that may be assigned this report)*
d.	

10. AVAILABILITY/LIMITATION NOTICES

Distribution of this document is unlimited.

11. SUPPLEMENTARY NOTES	12. SPONSORING MILITARY ACTIVITY
	Office of Naval Research

13. ABSTRACT

[See Page Following]

DD FORM 1 JAN 64 1473

UNCLASSIFIED

Security Classification

14. KEY WORDS	LINK A		LINK B		LINK C	
	ROLE	WT	ROLE	WT	ROLE	WT
Sun						
Solar X-Rays						
Solar Radio Noise						
Solar Flares						

INSTRUCTIONS

1. ORIGINATING ACTIVITY: Enter the name and address of the contractor, subcontractor, grantee, Department of Defense activity or other organization *(corporate author)* issuing the report.

2*a*. REPORT SECURITY CLASSIFICATION: Enter the overall security classification of the report. Indicate whether "Restricted Data" is included. Marking is to be in accordance with appropriate security regulations.

2*b*. GROUP: Automatic downgrading is specified in DoD Directive 5200.10 and Armed Forces Industrial Manual. Enter the group number. Also, when applicable, show that optional markings have been used for Group 3 and Group 4 as authorized.

3. REPORT TITLE: Enter the complete report title in all capital letters. Titles in all cases should be unclassified. If a meaningful title cannot be selected without classification, show title classification in all capitals in parenthesis immediately following the title.

4. DESCRIPTIVE NOTES: If appropriate, enter the type of report, e.g., interim, progress, summary, annual, or final. Give the inclusive dates when a specific reporting period is covered.

5. AUTHOR(S): Enter the name(s) of author(s) as shown on or in the report. Enter last name, first name, middle initial. If military, show rank and branch of service. The name of the principal author is an absolute minimum requirement.

6. REPORT DATE: Enter the date of the report as day, month, year; or month, year. If more than one date appears on the report, use date of publication.

7*a*. TOTAL NUMBER OF PAGES: The total page count should follow normal pagination procedures, i.e., enter the number of pages containing information.

7*b*. NUMBER OF REFERENCES: Enter the total number of references cited in the report.

8*a*. CONTRACT OR GRANT NUMBER: If appropriate, enter the applicable number of the contract or grant under which the report was written.

8*b*, 8*c*, & 8*d*. PROJECT NUMBER: Enter the appropriate military department identification, such as project number, subproject number, system numbers, task number, etc.

9*a*. ORIGINATOR'S REPORT NUMBER(S): Enter the official report number by which the document will be identified and controlled by the originating activity. This number must be unique to this report.

9*b*. OTHER REPORT NUMBER(S): If the report has been assigned any other report numbers *(either by the originator or by the sponsor)*, also enter this number(s).

10. AVAILABILITY/LIMITATION NOTICES: Enter any limitations on further dissemination of the report, other than those imposed by security classification, using standard statements such as:

(1) "Qualified requesters may obtain copies of this report from DDC."

(2) "Foreign announcement and dissemination of this report by DDC is not authorized."

(3) "U. S. Government agencies may obtain copies of this report directly from DDC. Other qualified DDC users shall request through _____."

(4) "U. S. military agencies may obtain copies of this report directly from DDC. Other qualified users shall request through _____."

(5) "All distribution of this report is controlled. Qualified DDC users shall request through _____."

If the report has been furnished to the Office of Technical Services, Department of Commerce, for sale to the public, indicate this fact and enter the price, if known.

11. SUPPLEMENTARY NOTES: Use for additional explanatory notes.

12. SPONSORING MILITARY ACTIVITY: Enter the name of the departmental project office or laboratory sponsoring *(paying for)* the research and development. Include address.

13. ABSTRACT: Enter an abstract giving a brief and factual summary of the document indicative of the report, even though it may also appear elsewhere in the body of the technical report. If additional space is required, a continuation sheet shall be attached.

It is highly desirable that the abstract of classified reports be unclassified. Each paragraph of the abstract shall end with an indication of the military security classification of the information in the paragraph, represented as *(TS)*, *(S)*, *(C)*, or *(U)*.

There is no limitation on the length of the abstract. However, the suggested length is from 150 to 225 words.

14. KEY WORDS: Key words are technically meaningful terms or short phrases that characterize a report and may be used as index entries for cataloging the report. Key words must be selected so that no security classification is required. Identifiers, such as equipment model designation, trade name, military project code name, geographic location, may be used as key words but will be followed by an indication of technical context. The assignment of links, roles, and weights is optional.

ABSTRACT

A study of the histories of solar flares observed at 2 cm at the North Liberty Radio Observatory of the University of Iowa and observed at x-ray wavelengths with Mariner V (2-9 A) and Explorers 33 and 35 (2-12 A) shows that "post-burst increase" and "gradual rise and fall" events are concurrent microwave and soft x-ray phenomena. The correlation between the x-ray flux and the radio flux is high but non-linear. The character of the correlation is consistent with a thermal flare theory in which the volume emissivity at x-ray wavelengths is of the spectral form $(dE/d\nu) \sim \exp(-h\nu/kT)$ and the radio flux is from the same region which is optically thick with a temperature T. The correlation yields the peak flare temperature, T_p, and the flare solid angle in terms of the fractional increase in temperature relative to the peak temperature, $F = \delta T/T_p$. Comparing flare sizes with those obtained by other means (e.g., x-ray telescopes) shows $F > 0.2$. If free-free emission is assumed responsible for both the x-ray and the radio emissions, an $F \sim 0.5$ is consistent with the initial assumptions while an $F \sim 1.0$ is not. Thus, temperatures typically double during a flare. Of twenty cases studied, an $F = 0.5$ yielded a mean peak temperature of 4 million degrees Kelvin and a mean effective diameter of 32 arc seconds.